# Fundamental and harmonic emission from the rear side of a thin overdense foil irradiated by an intense ultrashort laser pulse

K. Eidmann, T. Kawachi, A. Marcinkevičius, R. Bartlome, G. D. Tsakiris, and K. Witte
*Max-Planck Institute für Quantenoptik, Hans-Kopfermann Str. 1, D-85748 Garching, Germany*

U. Teubner
*Institut für Experimentelle Physik, Universität Duisburg-Essen, Universitätsstr. 5, D-45117 Essen, Germany*
(Received 28 April 2005; published 26 September 2005)

The emission of fundamental and harmonic radiation from the rear side of thin foils in the thickness range 50–460 nm irradiated by intense frequency doubled Ti:sapphire laser pulses of the duration of 150 fs and intensities up to a few $10^{18}$ W/cm$^2$ was investigated. Following up a previous study of the rear side harmonic emission [Teubner *et al.*, Phys. Rev. Lett. **92**, 185001 (2004)], we measured the emission efficiencies, polarization properties, and the spectral shapes of the fundamental frequency and the second harmonic. Rear side emission is only observed when the obliquely incident laser light is *p*-polarized. Particle-in-cell (PIC) simulations indicate that the foils remain strongly overdense during the interaction with the laser pulse and that the rear side emission is caused by energetic electron bunches which are generated at the front side by resonance absorption. They are accelerated into the foil and drive strong plasma oscillations at the fundamental and higher harmonic frequencies.

DOI: 10.1103/PhysRevE.72.036413 PACS number(s): 52.38.−r, 42.65.Ky, 52.25.Os

## I. INTRODUCTION

The recent progress in generating intense ultrashort laser pulses of sub-ps duration has lead to a plenty of nonlinear effects in the laser plasma interaction at high intensities [1–3]. One important process is the generation of optical harmonics by irradiating solid targets with intense laser pulses. Originally observed with long $CO_2$ laser pulses of ns duration [4,5], this effect has recently been investigated in many experiments with ultrashort laser pulses [6–13]. In addition, substantial theoretical work has been done, mainly on the basis of particle in cell (PIC) calculations [14,15]. The interest in this process is caused by the fact that it gives insight into the complex processes occurring during the laser plasma interaction at high intensities. Also, the application as a bright coherent XUV light source is very promising, because with solid targets there are no principal intensity limitations as it is the case in harmonic generation with gases [16]. Presently, even the generation of sub-fs x-ray pulses is under discussion [17].

Usually, harmonics from solid targets are studied in reflection from the sharply edged overdense plasma layer in front of the target, which is set into an oscillatory motion under the influence of the intense laser field. As a consequence, the phase of the reflected light is modulated leading to harmonics. This "oscillating mirror" model was quite successful to explain the high order harmonic emission [14,18]. Recently, we investigated the emission of harmonics from thin foils with the thickness of a laser wavelength $\lambda_0$ (=395 nm) and below [19], which were irradiated under oblique incidence with *p*-polarized laser light. As shown schematically in Fig. 1(a), we measured in addition to the reflected harmonics also the emission taking place at the rear side of the foil in the direction of the incident laser light. One motivation of this experiment was to look for transmitted harmonics, which are expected to appear at frequencies above the plasma frequency $\omega_p$ of the solid foil, but should be strongly suppressed below $\omega_p$ [20–22]. It was proposed to use this cutoff towards low frequencies as a diagnostic to measure the electron density of the ionized foil. By using gas harmonics as a probe the existence of such a low frequency cutoff had been demonstrated [23].

The result of our experiment was quite surprising: Instead of transmitted harmonics expected above the plasma frequency $\omega_p$ of the dense foil, we observed just the opposite, namely low order harmonics including the fundamental with an intensity strongly increasing with decreasing order [Fig. 1(b)]. Because we used clean frequency doubled laser pulses with a low prepulse level, we were sure, that the foil remained overdense with a density close to solid density dur-

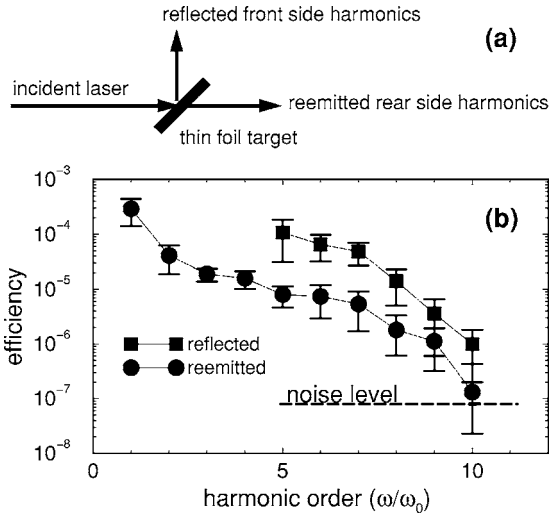


FIG. 1. (a) Scheme of the experiment. (b) Measured reflected and re-emitted harmonics [19].

 

ing the interaction (the plasma frequency of the solid foil is $\omega_p/\omega_0 \approx 9$, where $\omega_0$ is the laser frequency). Thus we can exclude the transmission of harmonics generated at the front side (in the following we denote the rear side harmonics as "re-emitted" harmonics). We explained the re-emission of harmonics by energetic electron bunches which are created in the interaction region and pass through the dense foil. They excite plasma oscillations in the bulk plasma of the dense foil at positions where the local plasma frequency is in resonance with a multiple of $\omega_0$ (i.e., where $\omega_p \approx q\omega_0$, $q=1,2,\ldots$). Since this occurs in an inhomogeneous plasma, reemission of harmonics can take place. As will be discussed later on, this mechanism for harmonic production by resonances in the bulk of the plasma is different from the mirror model. The fact that we did not observe the cutoff to the low frequency side as predicted in the references [20,21] is caused by the different conditions used in the PIC calculations and the experiment. In particular, in the simulations [20,21] the laser intensity $I$ was larger ($a_0 > 1$) than in our experiment where $a_0 \leqslant 0.5$. Here $a_0$ is the normalized vector potential given by

$$a_0^2 = I\lambda_0^2/[1.37 \times 10^{18}(\mathrm{W/cm^2})\mu\mathrm{m}^2].$$

Because the re-emission of harmonics is an interesting new phenomenon we have studied it further. In our previous study [19] we used a transmission grating spectrograph, which is appropriate for the higher order harmonics. The presence of low order harmonics with $q \leqslant 2$ was concluded from the diffraction pattern caused by the support structure [24]. In this paper we present in Sec. II more detailed measurements of the re-emitted fundamental light at $\lambda_0 = 396$ nm and the second order harmonic at 198 nm by using optical diagnostics. We measured the conversion efficiencies and the spectra of these harmonics at different intensities and Al foil thicknesses. We also determined the polarization properties of the reemitted fundamental light. In addition to the experimental results, we have performed extensive PIC simulations, which help to understand the observed reemission from the rear side of overdense foils and are described in Sec. III.

We finally note, that the observations reported here are different from other effects leading to the emission of fundamental or harmonic light at the rear side of thin foils. Recently several authors observed coherent transition radiation at the fundamental frequency [25,26] and the harmonic frequency [27]. It was attributed to energetic electrons, which propagate from the interaction region to the rear side and generate transition radiation when they traverse the rear foil-vacuum interface. For the reemitted light observed in our experiment we can exclude transition radiation, because it is expected in the direction of the electrons driven by the electric field, which is along the normal of the foil as will be discussed in Sec. III. In contrast, the re-emitted harmonics are observed in the direction of the incident laser light [see Fig. 1(a)]. Also we can exclude phenomena such as anomalous transparency [28] or hole burning [29] which occur at very high intensities in the relativistic regime ($a_0 \gg 1$) and which are much larger than the modest intensities of this experiment ($a_0 \leqslant 0.5$).

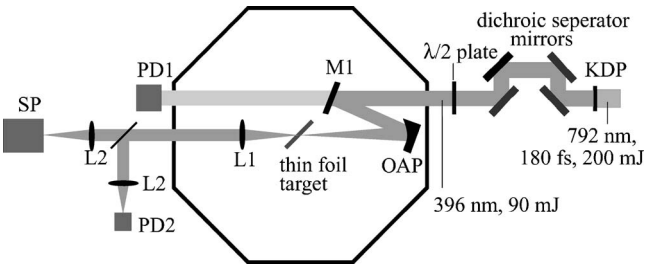


FIG. 2. Experimental setup.

## II. EXPERIMENT

### A. Experimental setup

The setup of the experiment is shown in Fig. 2. The experiment was performed with the 2-TW version of the ATLAS Ti:sapphire laser facility at the Max-Planck Institute for Quantum Optics (MPQ) [30]. It delivers at a repetition rate of 10 Hz pulses of a duration of 130 fs, an energy of up to 230 mJ, a central wavelength of 792 nm, and a beam diameter of about 63 mm (at 86.5% level). The pulse-contrast ratio was about $1{:}10^8$ at $t > 2$ ns and $1{:}10^4$ at 1 ps$< t <2$ ns. We improved the pulse-contrast ratio by frequency doubling using a 2 mm thick KDP crystal plate of 65 mm diameter. To optimize the conversion efficiency by reducing the group-velocity mismatch, we increased the pulse duration of ATLAS-2 to 180 fs by detuning the compressor. We achieved a conversion efficiency of 45% at an intensity of 30 GW/cm$^2$ at 792 nm. From the pulse contrast ratio at 792 nm wavelength, the contrast ratio of the second harmonic at 398 nm was estimated to be $1{:}10^{10}$ at $t > 2$ ns, and $1{:}10^8$ at 1 ps$< t <2$ ns [31]. A high pulse contrast ratio is important for avoiding early expansion of the thin foil target by prepulses and for producing a steep density gradient, which is necessary for efficient harmonic generation [9,13]. The frequency doubled light was separated from the unconverted light by four dielectric mirrors, which reflect >99% at 396 nm and transmit >99% at 792 nm. Thus the 792 nm light was suppressed by a factor of $10^8$.

After separation the 396 nm laser light (in the following text, we will denote the frequency doubled light at 396 nm as "fundamental") was directed into a vacuum chamber, where it was reflected by a dielectric mirror, M1, with a reflection coefficient of 99% and focused onto the target by a dielectric off-axis parabolic mirror, OAP, with an f-number of $F^{\#} = f/2.5$. Beam leaking through the mirror M1 was used for monitoring the input laser energy with a calibrated PIN photo-diode, PD1. The focus at the target position was checked by a $F^{\#} = f/2$ lens which creates a 55 times magnified image of the focal intensity distribution on a 14-bit CCD camera. The focal spot was a single peak of 5 $\mu$m diameter containing 50% of the energy. This yields a maximum average intensity of $1.5 \times 10^{18}$ W/cm$^2$, while the peak intensity at the center was about $6 \times 10^{18}$ W/cm$^2$.

The targets were free standing aluminum foils with a thickness ranging from 50 nm to 460 nm. The foils were put on a $50 \times 50$ mm target holder plate with 60 holes of 1 mm diameter on it. The angle of incidence of the laser was 45° with respect to the surface normal. By means of a $\lambda/2$-plate

*p*- or *s*-polarized light could be used. The target holder was mounted on an *xyz* translation unit and was moved between consecutive shots to always present a fresh surface. In all experiments the laser was operated under a single shot mode. The best focus on the target was controlled by maximizing the x-ray emission, which was measured by a scintillator after filtering with a thin foil. The cut-off energy for this filter set was about 40 keV. The shot-to-shot fluctuation of the scintillator signal was less than 10%.

The emission from the rear side of the foil target was collected and collimated by a lens, L1, and directed out of the vacuum chamber. The diameter of the lens L1 was sufficiently large to cover the full aperture of the incident laser beam ($F^{\#}=f/2.5$). We checked that the reemitted fundamental light is emitted into a solid angle which is close to that of the incident light. Thus, we are sure that the lens L1 collects the entire reemitted fundamental light. The collimated light was divided into two beams by a beam splitter. The reflected beam was focused by the lens L2 onto the PIN photodiode PD2, which measured the re-emitted pulse energy. The transmitted beam was focused by a lens with a focal distance of 500 mm, L2, at the entrance slit of a spectrometer (ORIEL, MS125) equipped with a 1200 grooves/mm grating. The inverse linear dispersion of this spectrometer was 0.7 nm/mm at 400 nm, i.e., the spectral resolution $\Delta\lambda/\lambda$ was $\approx$0.07 nm for the 100 $\mu$m-wide entrance slit. The wavelength of the spectrometer was calibrated by means of a Hg and Ar standard lamp (UVP Inc. type 90-0012). The spectra were measured in a single shot together with the incident energy and the re-emitted fundamental energy obtained from the signals of the diodes PD1 and PD2.

### B. Experimental results

#### *1. Conversion efficiency*

The conversion efficiency of the reemitted fundamental and the second harmonic is defined as the output energy at the corresponding wavelength divided by the input laser energy. To avoid saturation of the two PIN photodiodes during the measurement of the fundamental light, calibrated neutral density filters were used. Contributions from the second harmonic were completely suppressed by these filters due to their strong absorption around 200 nm. For the measurement of the conversion efficiency of the second harmonic, we eliminated the contribution from the fundamental by means of two dielectric mirrors (not shown in Fig. 2), which were installed between the lenses L1,2 and which have a peak reflectivity at 197 nm and a high transmissivity at 396 nm. In addition, an interference filter for the second harmonic (bandwidth was about 10 nm) was placed in front of photodiode PD2. Its bandwidth was about 10 nm, which is large enough for complete transmission of the second harmonic. These measures result in a suppression ratio of about $10^6$ for the fundamental. Since all higher-order harmonics ($q>2$) were in the vacuum ultraviolet region, the contribution from these harmonics is negligibly small.

In Fig. 3(a) the conversion efficiency of the fundamental light and the second harmonic is plotted as a function of the target thickness at a fixed incident intensity of 8 $\times 10^{17}$ W/cm$^2$. We also included the results from our previous measurements of the conversion efficiency of the seventh harmonic [19]. The conversion efficiencies of the fundamental and the second harmonic do not significantly change up to a thickness of 200 nm, but above 200 nm they decrease strongly with the foil thickness. In contrast, the decrease of the seventh harmonic sets in immediately at 50 nm and drops above 100 nm below the detection limit.

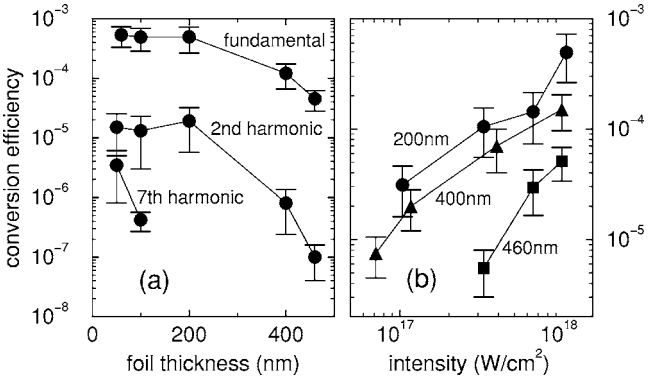


FIG. 3. Measured conversion efficiency of re-emitted light. (a) Dependence of the re-emitted fundamental, second and seventh harmonic on the foil thickness at the maximum intensity of the experiment ($1.5\times10^{18}$ W/cm$^2$). (b) Dependence of the fundamental conversion on the incident laser pulse intensity for the three different foil thicknesses.

Figure 3(b) shows the measured conversion efficiency of the re-emitted fundamental as a function of the laser intensity at a fixed foil thicknesses of 200 nm, 400 nm, and 460 nm. The laser intensity was changed by reducing the incident energy, while the foil was always kept in the focus. For all foil thicknesses the conversion efficiency increases in the intensity range under consideration. Note, that the smallest measured conversion efficiency for the 200 nm thick aluminum foil at the fundamental wavelength was still more than five orders of magnitude higher than classical transmission of the light through the metal foil (see Sec. III).

The data points in Fig. 3 represent averages over a number of shots. The error bars are mainly caused by shot to shot fluctuations of the output signal, which strongly depend on surface conditions of the foil.

#### *2. Spectra of re-emitted light*

We have investigated spectra of the re-emitted fundamental light and second harmonic at different foil thicknesses and irradiation intensities. Figure 4(a) shows the influence of the incident laser intensity and Fig. 4(b) of the foil thickness on the re-emitted fundamental light spectra. For comparison, we have also plotted the spectrum of the incident laser light, which has a full width at half maximum (FWHM) of $\Delta\omega/\omega_0=0.0043$ (or $\Delta\lambda=1.7$ nm). The re-emitted light spectra are significantly broader than the incident light spectrum. As will be discussed in Sec. III, this indicates that the duration of the re-emitted pulse is shorter than the duration of the incident laser pulse. In addition, the spectra of the re-emitted light show a "red" wing on the low frequency side, which becomes more and more pronounced, when the intensity is

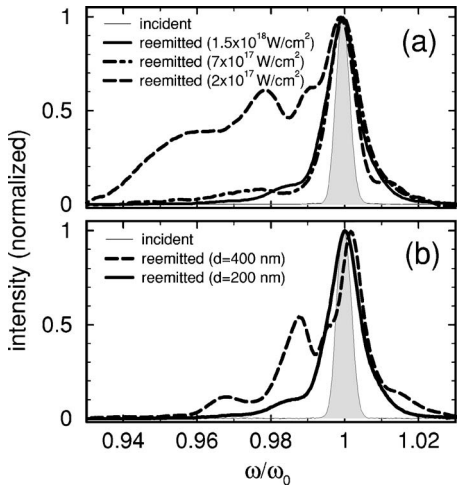


FIG. 4. Measured spectral line shapes of the re-emitted fundamental. (a) Spectra at three different incident laser intensities and fixed foil thickness (=200 nm). (b) Spectra at two different foil thicknesses and fixed incident intensity ($=1.5\times10^{18}$ W/cm$^2$). In addition to the re-emitted spectra the incident spectrum is displayed.

reduced [Fig. 4(a)] or when the foil thickness is increased [Fig. 4(b)].

We also measured spectra of the second harmonic. Because of its low conversion, the spectrometer signal was close to the detection limit. Thus we could not systematically study how the spectra depend on intensity and foil thickness. For a 200 nm thick foil and the maximum incident intensity ($1.5\times10^{18}$ W/cm$^2$) the typical FWHM of the re-emitted harmonic was 3–4 nm or $\Delta\omega/2\omega_0=1.5\%-2\%$.

#### *3. Polarization properties*

The results presented so far in Figs. 3 and 4 have been obtained with *p*-polarized incident laser light. In previous experiments it was found that efficient harmonic production in reflection was achieved only with *p*-polarized incident laser light [9]. We have checked if the polarization of the incident light is also important for the re-emitted light. For this purpose we alternatively irradiated the foil target with *p* and *s*-polarized light, and compared the two spectra of the re-emitted fundamental light. The polarization of the incident beam could easily be changed by rotating the $\lambda/2$ plate (see Fig. 2). The foil thickness was 400 nm and the laser intensity was at the maximum ($\approx10^{18}$ W/cm$^2$). We found that for *s*-polarized incident light the reemission signal was below the detection limit, which means that it was at least 400 times smaller than for *p*-polarized incident light. This result also indicates, that the foil remains overdense during irradiation.

In addition, we checked the polarization of the reemitted fundamental light, when the incident light was *p*-polarized. To this end, a Wollaston prism with a separation angle of 0.2° was positioned between the lenses L1 and L2. In this way one obtains two foci for the horizontally and vertically polarized components at the entrance slit of the spectrometer. They are separated in the direction perpendicular to the slit. Therefore the entrance slit was removed to allow for the passage of both polarization components which are then imaged by the spectrometer separately on the detector plane. The spectrometer sensitivity for different polarization components was checked by means of a He-Ne laser at 633 nm the polarization direction of which was 45°. Using this setup, we measured the polarization of the reemitted fundamental light in the case of a 400 nm thick foil at the maximum laser intensity ($\approx1.5\times10^{18}$ W/cm$^2$). The vertical polarization component (*s*-polarized light) could not be seen, what means that the *p*-polarization of the incident light is completely conserved in the re-emitted light.

## III. SIMULATION RESULTS AND DISCUSSION

### A. State of the foil and classical transparency

For the interpretation of the experimental results it is important to know the state of the foil when the main pulse arrives. Since the prepulse level of the frequency doubled pulse is very low, it is expected that the foil targets remain strongly overdense. To confirm this we have performed hydrodynamic calculations with the MULTI-fs code.[32] As input we used the temporal shape of the laser pulse including the weak pedestal.[9] We find only very little expansion. At the time ($t=t^*$) when the main pulse starts (150 fs before the main pulse) the foils are still at solid state density (=2.7 g/cm$^2$ for Al) even for the smallest foil thickness (50 nm) used in this experiment. The typical gradient length (defined by $L_c=n_e/\nabla n_e$ taken at $n_e=n_c$, $n_c=7.3\times10^{21}$ cm$^{-3}$) at the front side is still very steep (typically $L_c=0.1\lambda_0$). The temperature in the foil is at $t=t^*$ already quite high (close to 2 keV for the 50 nm foil) due to a heat wave propagating quickly through the foil. Thus we can assume that the foil is in a highly ionized state when the high intensity interaction starts. As a result of the PIC calculations presented below, the foil also remains during the short duration of the main pulse still at a high density close to the solid state density.

Under these conditions the classical transparency of the foil [$T_c=\exp(-d_f/d_s)$ with $d_f$ and $d_s$ the foil thickness and skin depth, respectively], is very low. For the thinnest foil ($d_f=50$ nm), $T_c$ for the fundamental and the second harmonic does not exceed values of a few times $10^{-7}$, which is considerably less than the rear side emission observed experimentally. Considering that the foil may slightly expand during the interaction, $T_c$ gets even smaller, because $d_s \propto c/\omega_p \propto 1/\sqrt{n_e}$ while $d_f \propto 1/n_e$. The latter proportionality holds for a one-dimensional expansion which is a reasonable assumption for the thin foils used by us with thicknesses which are small compared to the laser spot size. From these considerations we conclude that classically transmitted light is a negligible contribution to the experimentally observed re-emitted light.

### B. PIC simulations

At the high intensities of this experiment kinetic effects are very important. We have performed numerical simulations with the collisionless one-dimensional LPIC code developed by Lichters *et al.* [14,33]. The code allows for ob-

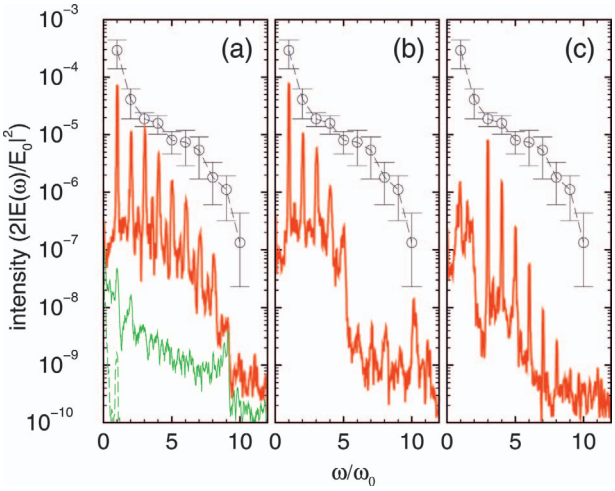


FIG. 5. (Color) Intensity of the calculated re-emitted spectra (red lines) at different densities: $n_e/n_c$=84 in (a), =27 in (b), and =4.2 in (c). Foil thicknesses are 0.2λ in (a), 0.6λ in (b), and 4λ in (c) corresponding to a fixed mass per area. The green line in (a) is the calculated re-emitted spectrum for incident *s*-polarized light (the dashed and solid green lines are the *p*- and *s*-polarized components, respectively). To compare the shape of simulated spectra with the experiment, we have added into each diagram (a, b, and c) the measured conversion efficiencies at the different orders (the open circles with error bars, allready shown in Fig. 1).

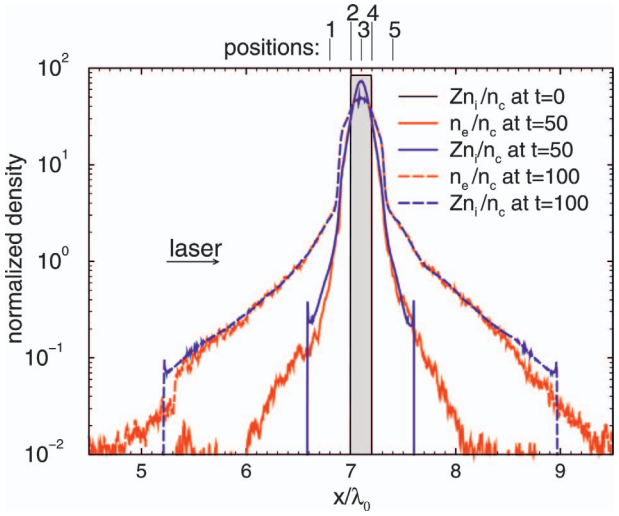


FIG. 6. (Color) Electron and ion density (normalized to $n_c$) at different times ($t$=0, 50, and 100, times are normalized to the period of the incident light, =1.33 fs at $\lambda_0$=400 nm). At the positions labeled by 1–5 the Fourier spectra of the density are plotted in Fig. 7.

lique incidence in the standard way by a Lorentz transformation into a moving frame [34].

The following simulations are done with a simulation box of length $15\lambda_0$ with the foil in the middle of the box. The foil had a sharp-edged gradient at the front and the rear side. Corresponding to the experiment the angle of incidence is 45° at *p*-polarization. The field amplitude of the incident pulse has a $\sin^2$ shape with a duration from foot to foot of 100 laser periods. All calculations are done with mobile ions.

In our previous paper we had already shown that the main trends of the measured re-emitted harmonic spectrum are well reproduced by the PIC simulations. To explain the measured re-emitted spectra a sufficiently high electron density is needed. This is demonstrated by Fig. 5, which displays the measured reemitted spectrum (of Fig. 1) together with the simulated spectrum for three different densities. In Fig. 5(a) the initial electron density $n_e/n_c$=84, which corresponds to solid Al assuming that the Al atoms are 10 times ionized. We did also runs at reduced density, namely at $n_e/n_c$=27 [Fig. 5(b)] and $n_e/n_c$=4.2 [Fig. 5(c)]. The areal mass density was kept constant, resulting in the different foil thicknesses given in the caption of Fig. 5. With the decreasing density the shape of the spectra changes in a characteristic way. The most prominent feature is a cutoff occurring at the plasma frequency of the dense foil, i.e., at

$$\omega_{\text{cutoff}}/\omega_0 \approx \omega_p/\omega_0 = (n_e/n_c)^{1/2}.$$

This yields the values $\omega_{\text{cutoff}}/\omega_0 \approx 9$, 5, and 2 for Figs. 5(a)–5(c), respectively. Above the cutoff transmitted harmonics appear which are rather weak for the higher density [Figs. 5(a) and 5(b)], but are very strong for the lowest density [Fig. 5(c)]. These harmonics at $q\omega_0 > \omega_p$ are caused by harmonics, which are generated at the front side of the foil according to the oscillating mirror mechanism and propagate through foil. The peak occurring at $\omega/\omega_0$ between 10 and 11 is attributed to emission at $2\omega_p$ [35].

For comparison also the measured reemitted spectrum (Fig. 1) is plotted (the comparison should be done only for the shape of the spectra, but not the absolute values, because the experimental data points represent the conversion efficiency, while in the case of the simulated spectra the intensity is plotted). It is evident, that the simulation at the highest density [Fig. 5(a)] is most suitable to describe the trend of the measurement. Thus we conclude, that during the time of the rear side emission the foil density is close to solid density.

The temporal development of the foil density is given by Fig. 6, which displays the electron and ion density at time $t$=0, at the peak of the incident pulse ($t$=50 periods) and at the end ($t$=100 periods, one period corresponds to 1.33 fs at $\lambda_0$=395 nm). It is seen that the foil starts to expand. However, during the pulse, the density in the middle of the foil is still high, well above $n_c$. At the front and rear side a density gradient builds up. At the end of the pulse ($t$=100) it is $L_c \approx 0.4\lambda$. At the plasma front electrons and ions separate leading to the typical structure with a step in the ion density and an electron cloud in front of the ion step (see, e.g., Ref. [36]).

The density shown in Fig. 6 undergoes in addition to the slow expansion a well defined rapid temporal modulation. This is demonstrated by Fig. 7. Here the Fourier spectrum of the density (taken over the total duration of the incident pulse) is plotted at 5 different positions in the foil plasma, namely at $x/\lambda_0$=6.8, 7, 7.1, 7.2, and 7.4 as indicated in Fig. 6. The density spectrum shows harmonics at integer multiples of the laser frequency $\omega_0$ with a strong peak near the local plasma frequency, i.e., at frequencies $q=\omega/\omega_0 \approx (n_e/n_c)^{1/2}$. In the middle of the foil $(n_e/n_c)^{1/2} \approx 9$, thus the

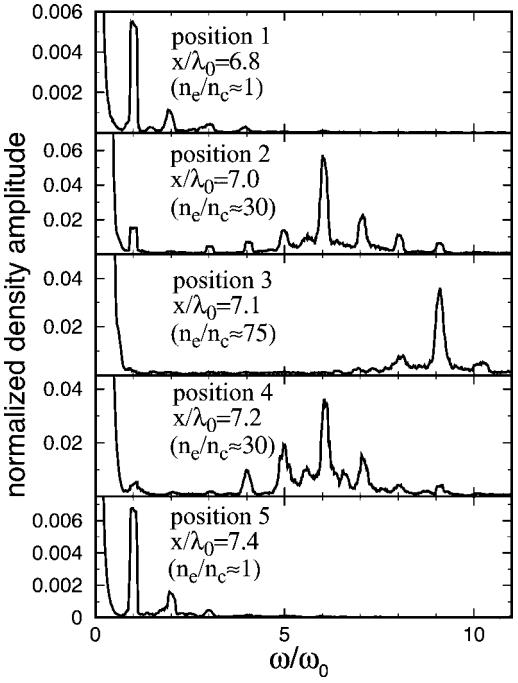


FIG. 7. Fourier transform of the electron density at the positions 1–5 indicated in Fig. 6. $n_e/n_c$ is the electron density (normalized to the critical density) at these positions. Note the change in the scale of the ordinate for the different positions. The plotted density amplitudes are normalized to the critical density.

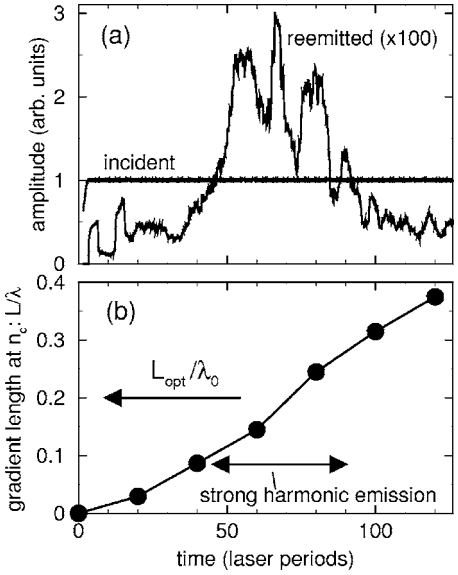


FIG. 8. (a) Intensity and (b) density scale length $L$ (at $n_e=n_c$) versus time for an incident pulse with constant intensity. In (b) the optimum gradient for resonance absorption is indicated.

ninth harmonic dominates. This oscillation leads to the emission of the ninth harmonic to the front and the rear side. Since no higher densities exist in the plasma, plasma oscillations $\omega/\omega_0 > 9$ cannot be excited. This explains the cutoff to the high frequency side observed in Fig. 5(a) at $q \approx 9$. At the front and the rear side of the foil (positions 1 and 5) $(n_e/n_c)^{1/2} \approx 1$. Consequently the fundamental oscillation ($q=1$) dominates.

This plasma oscillation at the rear side of the foil is responsible for the re-emitted fundamental light. The conversion of the electrostatic oscillation into light (forbidden in a homogeneous plasma) is attributed to the fact that the process occurs in a strongly inhomogeneous plasma. (The process may be considered as the reversal of the resonance absorption.) Our simulations show, that—associated with the plasma oscillations—electrical currents are flowing in the plane of the incident light. Both current components along and perpendicular to the target normal have the same resonant behavior as the electron density. An example was given in our previous paper (see Fig. 4 in Ref. [19]). These currents are the source of the harmonics emitted to the front and the rear side. Because the currents are modulated in the direction perpendicular to the normal of the foil by the same phase factor as the incident light, the light is emitted from the rear surface with the same direction and polarization as the incident light as is observed in the simulations and the experiment.

From this discussion it follows that for the intensities pertaining to this experiment different mechanisms for the harmonic production below and above $\omega_p$ are involved. Below $\omega_p$ the harmonics are generated by a resonant process, namely the excitation of plasma oscillations in the bulk of the plasma. In contrast, harmonics above $\omega_p$ are generated by the oscillating mirror mechanism, by which the plasma surface is driven to strong oscillations resulting in the emission of high order harmonics above $\omega_p$ [14]. At very high intensities this mechanism totally dominates the harmonic production and the apparent cutoff disappears.

### C. Importance of resonance absorption

Re-emitted light could only be observed, when the obliquely incident laser light was $p$-polarized. The same is found in the simulations. An example is shown in Fig. 5(a), where the rear side spectrum for $s$-polarized light is plotted, too. In agreement with the experiment, the fundamental light and the higher harmonics are suppressed by many orders of magnitude.

This behavior implies that resonance absorption is essential for the mechanism of generating re-emitted light. Efficient resonance absorption excited at a fixed angle of incidence requires an optimum density gradient length $L_{\mathrm{opt}}$ at $n_e=n_c$ which is given by [37]

$$(2\pi L_{\mathrm{opt}}/\lambda_0)^{1/3} \sin\theta = k,$$

where $k$ is a numerical constant with a value between 0.7 and 0.8 and $\theta$ the angle of incidence. For our conditions one obtains $L_{\mathrm{opt}} \approx 0.2\lambda_0$. In the simulation it takes some time until an optimum gradient has developed (compare Fig. 6). As a consequence the re-emission from the rear side starts after some delay. To make this more clear we have done a simulation for a pulse with the intensity constant in time, see Fig. 8. Indeed, the reemission sets in after some delay. It has some spiky structure, and it decreases after a while [Fig. 8(a)]. As shown by Fig. 8(b), the main re-emission takes place when the gradient length is close to its optimum value. This occurs only during a time interval which is shorter than

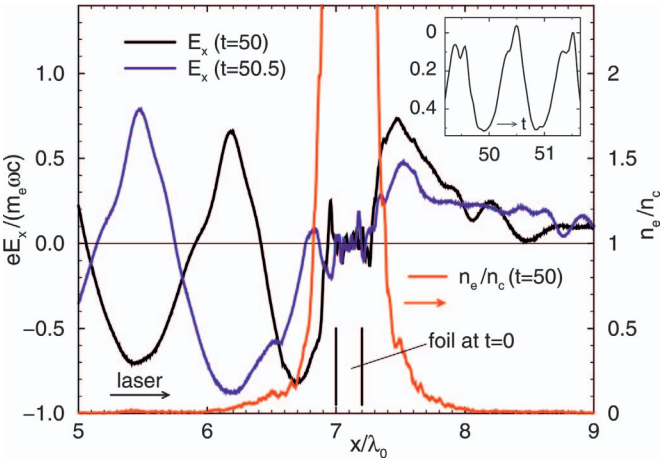


FIG. 9. (Color) The total electric field (in the direction of the normal of the foil) as a function of space at $t=50$ (black line) and a half period later ($t=50.5$, blue line). In addition the density is plotted (red line, ordinate at the right side). The inset shows the electric field as a function of time at the position $x/\lambda_0=7.2$, corresponding to $n_e=n_c$.

the total pulse length with the consequence that the re-emitted pulse is shorter than the incident laser pulse.

It is of interest to look at the electric field at a time when the optimum gradient length is reached. It is plotted in Fig. 9 at the time $t=50$ and a half laser period later at $t=50.5$. In addition, also the electron density is plotted at this time, showing that the position of the critical density is at $x/\lambda_0=7.2$. As expected, in the vacuum the field behaves like a standing wave and oscillates between a positive and negative value. However, near the critical density it oscillates only between zero and a negative value, as shown more clearly by the inset, where the electric field is plotted as a function of time (at the position of $n_c$). The lowering of the electric field to negative values is caused by the negative space charge of the electrons at the plasma front (see Fig. 6). The negative electric field periodically with the laser frequency accelerates electron bunches into the foil. These bunches drive the plasma oscillations at integer multiples of $\omega_0$ seen in Fig. 7.

### D. Comparison with experimental results

Finally we present a more direct comparison with the experimental results of Sec. II for comparison with the experimental results shown in Fig. 3. Figure 10 shows the calculated conversion efficiency of the re-emitted radiation.

In Fig. 10(a), where the conversion efficiency is plotted versus the foil thickness, we find a plateau for the fundamental and the second harmonic which is followed by a decrease at foil thicknesses above $\lambda_0\approx 0.5$. For the seventh harmonic the decrease already sets in for the thinnest foils. These trends are similar to the the experimental results shown in Fig. 3(a).

In Fig. 10(b) the intensity dependence is shown. We find an increase of the conversion efficiency up to $a_0\approx 1$. This corresponds to the experimental result [Fig. 3(b)], where we also observe an increase in conversion efficiency in the intensity range $5\times 10^{16}$ to $10^{18}$ W/cm$^2$, which range corresponds approximately to $0.1<a_0<0.5$. In the region above $a_0\approx 1$, which was not studied experimentally by us, the simulated conversion efficiency saturates at some value [Fig. 10(b)].

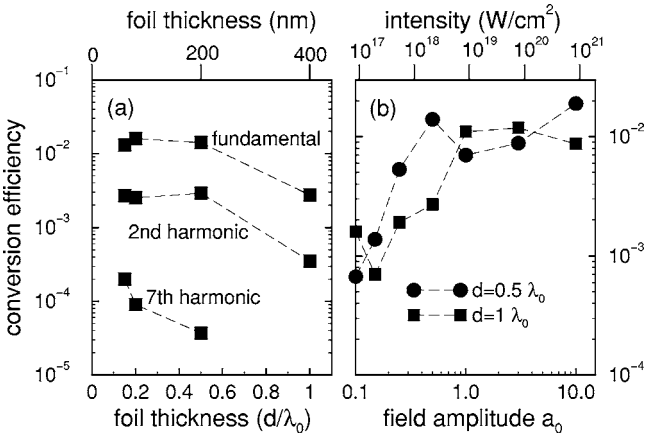


FIG. 10. Calculated re-emitted conversion efficiencies for comparison with Fig. 3. (a) Efficiencies of the fundamental, the second and seventh harmonics as a function of the foil thickness ($a_0=0.5$). (b) The re-emitted fundamental as a function of $a_0$ at different foil thicknesses.

Although the simulations reproduce roughly the trend of the experiment, there is a considerable discrepancy in the absolute value. The measured values of the conversion efficiency are by a factor 10–100 smaller than the calculated values. One reason can be attributed to the fact that the re-emission occurs only during a short time interval as demonstrated by Fig. 8. Since the incident laser pulse is longer in the experiment than in the simulations, the simulations may overestimate the conversion efficiencies. Also, it may be that the generation of re-emitted light takes place in a smaller central spot, where the intensity is high but the energy content smaller than the total incident energy. Of course, this is not considered by the one-dimensional simulation. Finally, we mention that collisions, which are not taken into account by the simulations, may dampen the plasma oscillations and weaken the re-emitted radiation.

We have also calculated the spectra of the reemitted fundamental. Corresponding to Fig. 4 they are displayed in Fig. 11(a) for two different intensities, and in Fig. 11(b) for two different foil thicknesses. Again we observe a similar trend as in the experiment. The reemitted spectra are in general broader than the incident spectra and their width increases with decreasing intensity and increasing foil thickness. Furthermore, the simulated spectra exhibit a "red" wing at the low frequency side, which was also seen in the experiment.

The broadening of the re-emitted spectrum is related to the fact that the re-emitted pulse is shorter than the incident pulse as discussed in the previous section. The spiking of the re-emitted pulse seen in Fig. 8 enhances the broadening further. The shift and the formation of a red wing may be attributed to phase modulation effects. They occur because the transfer of the signal from the laser irradiated side to the rear side of the foil occurs by electron bunches with velocities smaller than the light velocity. Thus, there is a delay between the excitation of the energetic electron bunches at the front

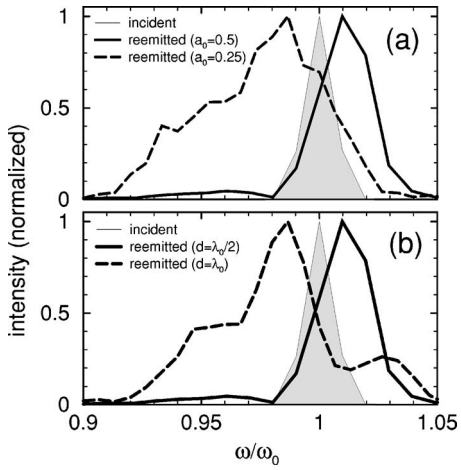


FIG. 11. Calculated spectral line shapes of the re-emitted fundamental. (a) Spectra at two different incident laser intensities and fixed foil thickness (200 nm). (b) Spectra at two different foil thicknesses and fixed incident intensity ($a_0$=0.5). In addition to the re-emitted spectra the incident spectra are displayed.

side and the excitation of the plasma oscillations at the rear side of the foil. Because we consider a very dynamic process, the delay may change because of the expansion of the foil (Fig. 6) and the change of the electron velocity during the re-emission.

## IV. SUMMARY

We have experimentally proven that intense harmonics including the fundamental are re-emitted from the rear side of thin foils irradiated under oblique incidence by a *p*-polarized high contrast ultrashort-pulse. In this paper we have presented a detailed study of the re-emitted fundamental and the second harmonic. We find that re-emitted light is observed already at low intensities corresponding to $a_0$=0.1. The conversion efficiency increases with the incident intensity and decreases with the foil thickness, but was still observed with foils of the thickness $1\lambda_0$. Efficient re-emission occurs only when the incident laser light is *p*-polarized. The spectrum of the re-emitted light is considerably broader than the spectrum of the incident laser light, in particular, at low intensities and thick foils, in which case we observed an enhanced wing on the red side.

The main trends of these results are in good agreement with one-dimensional PIC calculations. It is important to assume that the foil remains overdense during the interaction with the laser pulse. This follows from hydrodynamic calculations as well as from the PIC simulations, which are performed with immobile ions and do not show significant expansion of the foil below solid state density. Also, the shape of the measured harmonic spectrum agrees with the simulation only when the foil is close to solid state density. Thus the re-emitted light cannot be explained by classical transmission of the incident laser light and of the harmonics generated at the front side.

The fact that the reemission is observed only under *p*-polarization indicates that resonance absorption is essential. In fact, in the simulations efficient re-emission occurs only, if the gradient is optimal for resonance absorption which is the case over a short period of time while the foil expands. Thus the re-emitted pulse is shorter than the incident laser pulse resulting in a broader spectrum compared to the spectrum of incident pulse as is observed in the experiment.

The strong electric field associated with the resonance absorption accelerates energetic electrons into the foil which excite plasma oscillations in the foil at multiples of the laser frequency. Since the plasma oscillations take place in an inhomogeneous plasma, radiation at the harmonic frequencies is emitted to the front and the rear side. This resonant mechanism of harmonic emission below the plasma frequency of the dense foil is different from the moving mirror model, which is important for harmonic emission above the plasma frequency of the dense foil.

## ACKNOWLEDGMENTS

The authors would like to thank W. Fölsner for the preparation of the foil targets, and also thank ATLAS laser crew for their support. This work was supported in part by the European Communities in the framework of the European-IPP association and the Deutsche Forschungsgemeinschaft (DFG Grant Nos. TE 190/4-1 and TS82/1-1) and was also supported in part by a foundation of Japan Atomic Energy Scolarship.

[1] S. V. Bulanov, N. M. Naumova, and F. Pegoraro, Phys. Plasmas **1**, 745 (1994).
[2] P. Gibbon and E. Förster, Plasma Phys. Controlled Fusion **38**, 769 (1996).
[3] A. Pukhov, Rep. Prog. Phys. **66**, 47 (2003).
[4] N. H. Burnett, H. A. Baldis, M. C. Richardson, and G. D. Enright, Appl. Phys. Lett. **31**, 172 (1977).
[5] R. L. Carman, D. W. Forslund, and J. M. Kindel, Phys. Rev. Lett. **46**, 29 (1981).
[6] S. Kohlweyer, G. D. Tsakiris, C. G. Wahlstrom, C. Tillman, and I. Mercer, Opt. Commun. **117**, 431 (1995).
[7] D. von der Linde, T. Engers, G. Jenke, P. Agostini, G. Grillon, E. Nibbering, A. Mysyrowicz, and A. Antonetti, Phys. Rev. A **52**, R25 (1995).
[8] P. A. Norreys, M. Zepf, S. Moustaizis, A. P. Fews, J. Zhang, P. Lee, M. Bakarezos, C. N. Danson, A. Dyson, P. Gibbon, P. Loukakos, D. Neely, F. N. Walsh, J. S. Wark, and A. E. Dangor, Phys. Rev. Lett. **76**, 1832 (1996).
[9] M. Zepf, G. D. Tsakiris, G. Pretzler, I. Watts, D. M. Chambers, P. A. Norreys, U. Andiel, A. E. Dangor, K. Eidmann, C. Gahn, A. Machacek, J. S. Wark, and K. Witte, Phys. Rev. E **58**, R5253 (1998).

[10] A. Tarasevich, A. Orisch, D. von der Linde, T. Balcou, G. Rey, J. P. Chambaret, U. Teubner, D. Klöpfel, and W. Theobald, Phys. Rev. A **62**, 023816 (2000).
[11] I. Watts, M. Zepf, E. L. Clark, M. Tatarakis, K. Krushelnick, A. E. Dangor, R. J. C. R. M. Allott, R. J. Clark, D. Neely, and P. A. Norreys, Phys. Rev. Lett. **88**, 155001 (2002).
[12] U. Teubner, G. Pretzler, T. Schlegel, K. Eidmann, E. Förster, and K. Witte, Phys. Rev. A **67**, 013816 (2003).
[13] P. Monot, G. Doumy, S. Dubosz, M. Perdrix, P. D'Oliviera, F. Quérec, F. Réau, P. Martin, P. Audebert, J.-C. Gauthier, and J.-P. Geindre, Opt. Lett. **29**, 893 (2004).
[14] R. Lichters, J. Meyer-ter-Vehn, and A. Pukhov, Phys. Plasmas **3**, 3425 (1996).
[15] P. Gibbon, IEEE J. Quantum Electron. **33**, 1915 (1997).
[16] C. Spielmann, N. H. Burnett, S. Sartania, M. Schnürer, C. Kan, M. Lenzner, P. Wobrauschek, and F. Krausz, Science **278**, 661 (1997).
[17] S. Gordienko, A. Pukhov, O. Shorokhov, and T. Baeva, Phys. Rev. Lett. **93**, 115002 (2004).
[18] D. von der Linde and K. Rzàzewski, Appl. Phys. B: Lasers Opt. **63**, 499 (1996).
[19] U. Teubner, K. Eidmann, U. Wagner, F. Pisani, G. D. Tsakiris, K. Witte, J. M. ter Vehn, T. Schlegel, and E. Förster, Phys. Rev. Lett. **92**, 185001 (2004).
[20] P. Gibbon, D. Altenbernd, U. Teubner, E. Förster, P. Audebert, J.-P. Geindre, J.-C. Gauthier, and A. Mysyrowicz, Phys. Rev. E **55**, R6352 (1997).
[21] R. Lichters, "Relativistische Wechselwirkung Intensiver Kurzer Laserpulse mit Überdichten Plasmen: Erzeugung Hoher Harmonischer," dissertation, Technische Universität München, 1997.
[22] R. Hässner, W. Theobald, S. Niedermeier, H. Schillinger, and R. Sauerbrey, Opt. Lett. **22**, 1491 (1997).
[23] W. Theobald, R. Hässner, C. Wülker, and R. Sauerbrey, Phys. Rev. Lett. **77**, 298 (1996).
[24] U. Teubner, U. Wagner, U. Andiel, F. Pisani, K. Eidmann, G. D. Tsakiris, T. Schlegel, E. Förster, and K. Witte, Proc. SPIE **5196**, 146 (2003).
[25] J. J. Santos, F. Amiranoff, S. D. Baton, L. Gremillet, M. Koenig, E. Martinolli, M. Rabec LeGloahec, C. Rousseaux, D. Batani, A. Bernardinello, G. Greison, and T. Hall, Phys. Rev. Lett. **89**, 025001 (2002).
[26] J. Zheng, K. A. Tanaka, T. Sato, T. Yabuuchi, T. Kurahashi, Y. Kitagawa, R. Kodama, T. Norimatsu, and T. Yamanaka, Phys. Rev. Lett. **92**, 165001 (2004).
[27] S. D. Baton, J. J. Santos, F. Amiranoff, H. Popescu, L. Gremillet, M. Koenig, E. Martinolli, O. Guilbaud, C. Rousseaux, M. R. LeGloahec, T. Hall, D. Batani, E. Perelli, F. Scianitti, and T. E. Cowan, Phys. Rev. Lett. **91**, 105001 (2003).
[28] E. Lefebvre and G. Bonnaud, Phys. Rev. Lett. **74**, 2002 (1995).
[29] J. Fuchs, J. C. Adam, F. Amiranoff, S. D. Baton, P. Gallant, L. Gremillet, A. Héron, J. C. Kieffer, G. Laval, G. Malka, J. L. Miquel, P. Mora, H. P'epin, and C. Rousseaux, Phys. Rev. Lett. **80**, 2326 (1998).
[30] H. Baumhacker A. Böswald, H. Haas, K. J. Witte, U. Andiel, J. Bayerl, X. Dong, M. Dreher, K. Eidmann, M. Fischer, M. Hegelich, M. Kaluza, S. Karsch, G. Keller, G. Pretzler, H. Stehbeck, and G. Tsakiris, "Advanced Titanium Sapphire Laser ATLAS, volume MPQ-272 of Laboratory report," Max Planck Institut für Quantenoptik, 2002.
[31] A. Marcinkevičius, R. Tommasini, G. D. Tsakiris, K. J. Witte, E. Gaižauskas, and U. Teubner, Appl. Phys. B: Lasers Opt. **79**, 547 (2004).
[32] K. Eidmann, J. Meyer-ter-Vehn, T. Schlegel, and S. Hüller, Phys. Rev. E **62**, 1202 (2000).
[33] R. Lichters, R. E. W. Pfund, and J. M. ter Vehn, "LPIC++, a Parallel One-Dimensional Relativistic Electromagnetic Particle-In-Cell Code for Simulating Laser-Plasma-Interaction," volume MPQ-225 of Laboratory report, Max Planck Institut für Quantenoptik, 1997.
[34] A. Bourdier, Opt. Acta **26**, 1804 (1983).
[35] U. Teubner, D. Altenbernd, P. Gibbon, E. Förster, A. Mysyrowicz, P. Audebert, J.-P. Geindre, J.-P. Gauthier, R. Lichters, and J. Meyer-ter-Vehn, Opt. Commun. **62**, 217 (1997).
[36] P. Mora, Phys. Rev. Lett. **90**, 185002 (2003).
[37] W. L. Kruer, *The Physics of Laser Plasma Interactions* (Addison-Wesley, New York, 1988).